Heat capacity of α-AlH_3 and α-AlD_3 at temperatures up to 1000 K

2008 J. Phys.: Condens. Matter 20 275204

(http://iopscience.iop.org/0953-8984/20/27/275204)

J. Phys.: Condens. Matter **20** (2008) 275204 (10pp) doi:10.1088/0953-8984/20/27/275204

Heat capacity of α-AlH_3 and α-AlD_3 at temperatures up to 1000 K

V E Antonov[1,4], A I Kolesnikov[2], Yu E Markushkin[3], A V Palnichenko[1], Y Ren[2] and M K Sakharov[1]

[1] Institute of Solid State Physics, Russian Academy of Sciences, 142432 Chernogolovka, Moscow District, Russia
[2] Argonne National Laboratory, Argonne, IL 60439, USA
[3] Bochvar All-Russian Scientific Research Institute for Inorganic Materials, Rogova Street 5a, 123060 Moscow, Russia

E-mail: antonov@issp.ac.ru

Received 19 March 2008, in final form 9 May 2008
Published 2 June 2008
Online at stacks.iop.org/JPhysCM/20/275204

Abstract

The densest α modification of AlH_3 and AlD_3 is thermodynamically stable at high hydrogen pressures. At ambient pressure, α-AlH_3 and α-AlD_3 rapidly and irreversibly decompose to Al and H_2 or D_2 gas when heated to about 420 and 520 K, respectively. In the present paper, the heat capacities at constant volume (C_V) and at constant pressure (C_P) are calculated for α-AlH_3 and α-AlD_3 at a pressure of 1 atm and temperatures 0–1000 K using the phonon densities of states determined earlier by inelastic neutron scattering at helium temperatures (Kolesnikov *et al* 2007 *Phys. Rev.* B **76** 064302). The $C_P(T)$ dependence of AlH_3 is also measured at temperatures 6–30 K and 130–320 K and that of AlD_3 at 130–320 K in order to compensate for the scatter in the literature data and to improve the accuracy of the calculated C_V and C_P dependences at low temperatures.

S Supplementary data are available from stacks.iop.org/JPhysCM/20/275204

(Some figures in this article are in colour only in the electronic version)

1. Introduction

Aluminium trihydride α-AlH_3 has been intensely studied in the last few decades as one of the most promising materials for hydrogen storage, because it contains approximately twice as many hydrogen atoms per unit volume as liquid hydrogen and approximately five times more hydrogen per unit mass than the $FeTiH_2$ hydride used in hydrogen accumulators. In contrast to most other metal hydrides, hydrogen atoms in α-AlH_3 do not occupy any symmetrical interstitial positions in the metal lattice and have only two nearest metal neighbours. The unusual crystal structure of α-AlH_3 makes it an attractive object for the experimental investigation and modelling of lattice dynamics. Additionally, α-AlH_3 is dielectric [1] so its heat capacity is fully determined by the phonon density of states, $g(\omega)$, where ω is the phonon frequency. A comparison of the heat capacities determined experimentally and calculated from the $g(\omega)$ can provide an independent test for the correctness of the assumed interpretation of the complex vibrational spectrum of α-AlH_3. In its turn, the accurately constructed $g(\omega)$ spectrum can be used to calculate the heat capacity (and therefore all standard thermodynamical functions) of α-AlH_3 at temperatures much exceeding its decomposition temperature at ambient pressure, and this is useful for applications.

A good means to prove the consistency and integrity of results of studies on the lattice dynamics of metal hydrides is using compounds with different hydrogen isotopes, H and D, which have an atomic mass ratio as large as two. The spectra of phonon density of states were earlier constructed for both α-AlH_3 and α-AlD_3 using inelastic neutron scattering [2]. The heat capacity at constant pressure, C_P, was measured for α-AlH_3 at temperatures 30–298 K [3] and 15–300 K [4] and for α-AlD_3 at 15–340 K [4].

In the present work, we calculated the temperature dependences $C_V(T)$ of heat capacity at constant volume for α-AlH_3 and α-AlD_3 using the phonon densities of states

[4] Author to whom any correspondence should be addressed.

determined in [2]. Results of the calculation proved to be in a satisfactory agreement with the experimental $C_P(T)$ dependences from [3, 4], but a noticeable systematic departure was observed in rather wide temperature intervals. To ascertain the origin of this discrepancy, we additionally measured the $C_P(T)$ dependences of α-AlH_3 at 6–30 K and of both α-AlH_3 and α-AlD_3 at 130–320 K.

The difference between the $C_V(T)$ and $C_P(T)$ dependences of aluminium trihydride becomes significant at temperatures above 400 K. We calculated the corrections converting the $C_V(T)$ to $C_P(T)$ dependences for α-AlH_3 and α-AlD_3 at temperatures up to 1000 K by using the literature data on the compressibility of these compounds at room temperature [5, 6] and the coefficients of thermal expansion determined from our own x-ray diffraction measurements of the lattice parameters at 80–370 K.

2. Sample preparation and experimental details

The samples for the calorimetric and x-ray diffraction measurements were prepared from the same powders of α-AlH_3 and α-AlD_3 as the samples used in the inelastic neutron scattering experiments [2]. The AlH_3 powder with a grain size of 30 μm and a purity of 99.8 wt% was produced by a reaction of $LiAlH_4$ with $AlCl_3$ in ether solution at room temperature [7]. The AlD_3 powder with a grain size of 20 μm was prepared in the same way using the deuterium-substituted reagents. The main impurity in the deuteride was protium and the $H/(H + D)$ atomic ratio made up $1.5 \pm 0.5\%$ according to the spectral analysis.

The α-AlH_3 and α-AlD_3 samples used for the calorimetric studies were in the form of discs made by pressing the corresponding powder to 2 GPa at room temperature. The compression did not affect the crystal structure of the compounds and the resulting flat surface of the sample provided for its better thermal contact with the measuring cell. The heat capacity of α-AlH_3 at temperatures 6–30 K was measured with an accuracy of 2% by a laboratory-made highly sensitive relaxation microcalorimeter using a sample 2 mm in diameter and 0.2 mm thick (see [8] for more details). The heat capacity of α-AlH_3 and α-AlD_3 at temperatures 130–320 K was measured with a 5% accuracy by a Perkin-Elmer DSC-7 differential scanning calorimeter using a sample with a diameter of 5 mm and thickness of 1 mm.

X-ray diffraction patterns of α-AlH_3 and α-AlD_3 powder samples were collected at temperatures from 80 to 370 K using monochromated synchrotron radiation with a wavelength of $\lambda = 0.107\,857$ Å at beam line 11-ID-C at the Advanced Photon Source, ANL. The patterns were recorded on the MAR-345 image plate detector. Rietveld refinements were performed with the GSAS code [9].

3. Results and discussion

The 12-layer trigonal crystal structure of α-AlH_3 (space group $R\bar{3}m$) consists of equally spaced alternating planes of Al and H atoms stacked perpendicular to the c axis [10]. Columns of Al atoms and spirals of H atoms are parallel to the c axis and form a three-dimensional network of Al–H–Al bridges. Correspondingly, the phonon density of states of α-AlH_3 (figure 1(a)) is rather complex and consists of a band of low-frequency lattice vibrations at energies below 45 meV (three acoustic and three optical branches) and two well-separated bands of optical H vibrations, one between 61 and 135 meV (rotational motions and H–Al–H bond-bending deformations of corner-sharing AlH_6 octahedra; 12 modes in total) and another one at 174–263 meV (six modes of Al–H bond-stretching motions of H atoms) [2]. The interpretation of the spectrum is based on the results of *ab initio* calculations of [11]. The area under the curves representing the three vibrational bands in figure 1(a) is accordingly normalized to 6, 12 and 6 states.

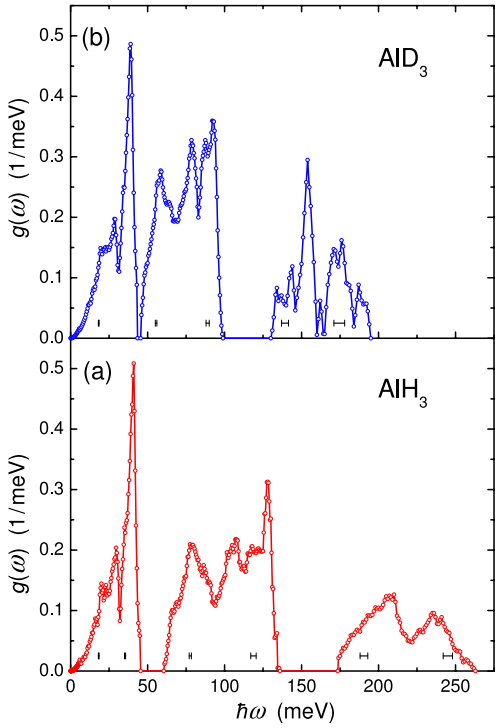

Figure 1. The densities of phonon states, $g(\omega)$, of α-AlH_3 (a) and α-AlD_3 (b) obtained from inelastic neutron scattering data [2]. The horizontal bars show the energy resolution of the INS spectra.

Figure 1(b) depicts the $g(\omega)$ spectrum of α-AlD_3 also constructed in [2]. The low-energy lattice modes virtually show a harmonic behaviour with respect to the isotopic substitution of H by D. That is, the low-energy part of the AlH_3 spectrum plotted as a function of $\hbar\omega/\sqrt{m_{AlD_3}/m_{AlH_3}} \approx \hbar\omega/\sqrt{33/30} \approx \hbar\omega/1.049$ well describes the $g(\omega)$ for translational vibrations of $Al(D_{1/2})_6$ units in the AlD_3 spectrum. The scaling factors for the lower and higher bands of optical hydrogen vibrations are 1.37 and 1.35, respectively. The departure of the scaling factors from the 'harmonic' ratio of $\sqrt{m_D/m_H} \approx \sqrt{2} \approx 1.41$ may partly result from the stronger interatomic forces in AlD_3 compared to those in AlH_3 due to the smaller interatomic distances [10].

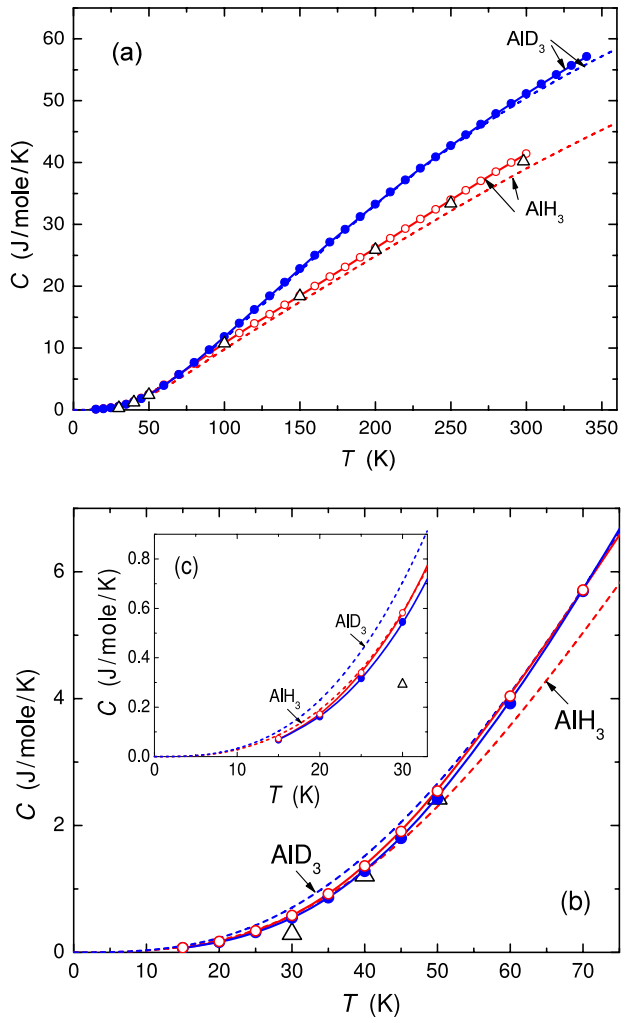

Figure 2. Temperature dependences of the heat capacities of α-AlH_3 and α-AlD_3. The experimental $C_P(T)$ data for AlH_3 are shown by the open triangles [3] and open circles [4] and the data for AlD_3 by the solid circles [4]. The lower and upper dashed curves, respectively, represent the $C_V(T)$ dependences for AlH_3 and AlD_3 calculated in this work using equation (1) and the $g(\omega)$ spectra constructed in [2] and displayed in figure 1.

The heat capacities of α-AlH_3 and α-AlD_3 were calculated as:

$$C_V(T) = \frac{R}{2}\int\left(\frac{\hbar\omega}{k_B T}\right)^2 g(\omega)n(\omega,T)\,[n(\omega,T)+1]\,\mathrm{d}\omega, \quad (1)$$

where $R = 8.314\ \mathrm{J\,mol^{-1}\,K^{-1}}$ is the universal gas constant, $k_B = 1.381\times10^{-23}\ \mathrm{J\,K^{-1}}$ is the Boltzmann constant and $n(\omega,T) = [\exp(\hbar\omega/k_B T)-1]^{-1}$ is the Bose factor. With the $g(\omega)$ spectra normalized to 24 states in total, this equation gives $C_V(T) \overset{T\to\infty}{\longrightarrow} 12R = 3R\times4$ per gram-mole of AlH_3 or AlD_3, in accordance with the Dulong and Petit law. The calculated $C_V(T)$ dependences are shown in figure 2 (dashed lines) together with the experimental $C_P(T)$ data available in the literature [3, 4].

In the temperature interval 0–360 K of figure 2, the C_V and C_P values for each of the two studied compounds can be compared directly, without any corrections, because the difference between the C_V and C_P is much smaller than the inaccuracy of the experimental and calculated data. As one can see from figures 2(a)–(c), the $C_V(T)$ curve calculated for AlD_3 nearly coincides with the experimental $C_P(T)$ at temperatures down to 70 K and deflects upward at lower temperatures. The slope of the $C_V(T)$ curve calculated for AlH_3 is smaller than that of the experimental $C_P(T)$ at all temperatures and the curves intersect at about 30 K.

It should be noticed, however, that the experimental data are not very precise. As seen from figures 2(b) and (c), the lowest 30 K point from [3] (open triangle) stands aside from all other data for AlH_3 and can rather be considered as a spurious observation. According to [4], the $C_P(T)$ curve for AlD_3 passes under the curve for AlH_3 at temperatures below 70 K (see figures 2(b) and (c)). At the same time, as discussed above, the phonon density of states of AlH_3 demonstrates nearly a harmonic behaviour with respect to the isotopic substitution of H by D. This necessitates the opposite behaviour of the $C_P(T)$ curves because the integral in equation (1) will be larger for AlD_3 than AlH_3 at any temperature. Assuming that the harmonic approximation is held, the relative error of the C_P measurements for AlH_3 and AlD_3 in [4] should have been no less than 10% at 70 K and increased to 20–25% at 30 K and lower temperatures.

The accuracy of determination of C_P (298.15 K) of AlH_3 declared in [4] was 0.3%, therefore the departure of our calculated $C_V(T)$ dependence for AlH_3 from the $C_P(T)$ measured in [4] at temperatures exceeding 200–250 K (figure 2(a)) might mean a discrepancy. In addition, the $g(\omega)$ spectra of AlH_3 and AlD_3 were experimentally determined only at energies above 5–6 meV [2] and this induced an element of uncertainty at temperatures up to 20–25 K in the calculated $C_V(T)$ dependences.

To have a reliable $C_P(T)$ dependence for AlH_3 at low temperatures, we measured it with an accuracy better than $\pm2\%$ in the interval from 6 to 30 K. To estimate the uncertainty in the experimental results of [3, 4] at moderate temperatures, we measured the $C_P(T)$ dependences for both AlH_3 and AlD_3 with an accuracy of $\pm5\%$ at 130–320 K.

3.1. Low and moderate temperatures

The obtained experimental $C_P(T)$ dependence for AlH_3 at 6 to 30 K is shown in figure 3 by open squares. It virtually coincides with the calculated $C_V(T)$ dependence (dashed curve) on the linear scale of this figure.

Figure 4 presents all available $C(T)$ data for α-AlH_3 and α-AlD_3 on a logarithmic scale. The lg C_P versus lg T dependence for AlH_3 measured in our work is nearly linear at temperatures from 30 to about 10 K and slightly deflects downward at lower temperatures. The linear portion of this dependence corresponds to $C_P \propto T^{2.70}$. As seen from figure 4, plotting the $C_P(T)$ data for AlH_3 and AlD_3 from [4] on the logarithmic scale produces linear dependences in the temperature interval 15–50 K. The dependences are nearly parallel and correspond to $C_P \propto T^{2.96}$.

The proportionality of low-temperature heat capacity to T^3 (the Debye behaviour) over a wide temperature interval is

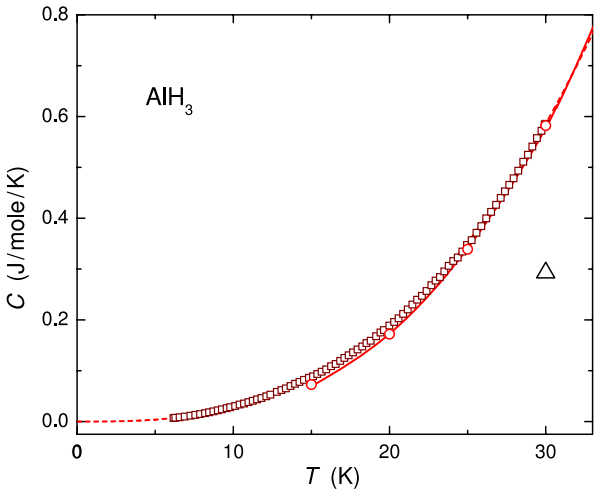

Figure 3. Heat capacity of α-AlH_3 as a function of temperature. The experimental $C_P(T)$ data are shown by the open squares (results of this work), open triangle [3] and open circles connected with a solid curve [4]. The dashed curve gives the calculated $C_V(T)$ dependence.

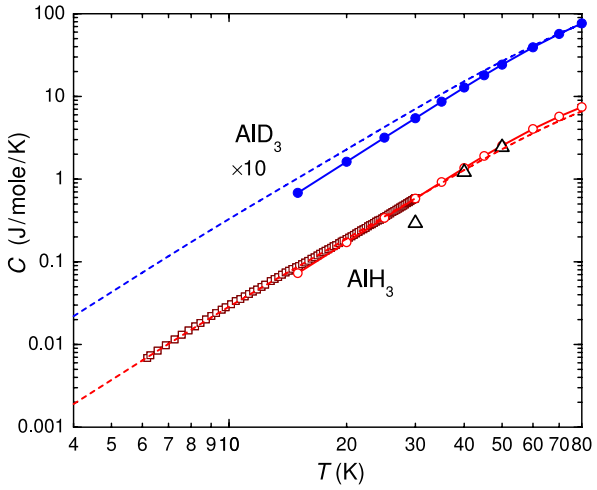

Figure 4. Double logarithmic plot of the heat capacity of α-AlH_3 and α-AlD_3 versus temperature. The open squares show the experimental $C_P(T)$ data of this work. Other notations as in figure 2. The data for AlD_3 are shifted vertically to avoid overlapping with the data for AlH_3.

typical of cubic non-metal compounds. The index of power for compounds like AlH_3 with complex, anisotropic structures should, as a rule, have a noticeably smaller value and can increase to a value of 3 only at very low temperatures [12]. In this connection, the $T^{2.70}$ dependence at temperatures down to 10 K obtained for AlH_3 in the present work is more plausible than $T^{2.96}$ from [4]. The increase in the exponent of our dependence at temperatures below 10 K can also be meaningful.

As the phonon density of states of AlH_3 was reliably measured only at energies down to 6 meV [2], we approximated it at lower energies by the Debye dependence $g(\omega) = A\omega^2$ and used A as a fitting parameter of equation (1) to reproduce our experimental dependence lg C_P versus lg T for AlH_3 at 6 K $< T <$ 30 K. It is the resulting $C_V(T)$ dependence that is shown in figures 2–4 by the dashed curves.

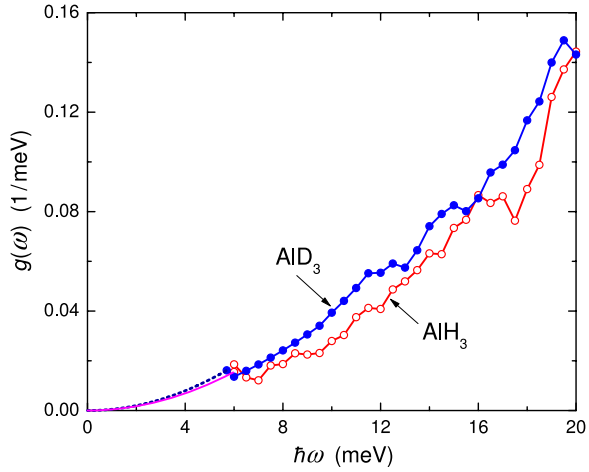

Figure 5. Smoothed spectra $g(\omega)$ of the phonon density of states for α-AlH_3 (open circles) and α-AlD_3 (solid circles) obtained by neutron spectroscopy [2] and the emulation of the spectra at $\hbar\omega < 6$ meV (solid and dashed line, respectively) by the Debye dependences $g(\omega) \propto \omega^2$, see text.

The optimized spectrum $g_{AlH3}(\omega)$ of AlH_3 at energies up to 6 meV is plotted in figure 5 by the solid line. The spectrum of AlD_3 in this energy interval (dashed line) was calculated as $g_{AlD3}(\omega) = g_{AlH3}(\omega/1.049)1.049$ in a harmonic approximation, saving the area under the $g(\omega)$ curve. The $C_V(T)$ dependence for AlD_3 generated by this 'composite' $g_{AlD3}(\omega)$ spectrum is presented in figures 2–4 by the corresponding dashed curves. Plotted on the logarithmic scale in figure 4, the calculated $C_V(T)$ dependences of both AlD_3 and AlH_3 are approximately linear at temperatures from 8 to 50 K and have nearly the same slope corresponding to $C_V \propto T^{2.75}$.

The $C_P(T)$ dependences for AlH_3 and AlD_3 measured at moderate temperatures of 130–320 K in the present work are shown in figure 6 by the thick solid curves. The accuracy ±5% of the measurement was presumably no worse than the accuracies of earlier studies [3, 4] in this temperature range.

As seen from figure 6, the experimental $C_P(T)$ dependences for AlD_3 constructed in our work and in [4] well agree with each other and the calculated $C_V(T)$ dependence passes between them. This suggests that the calculation accurately reproduces the $C_V(T)$ dependence of AlD_3 at temperatures up to about 350 K. The dependence should therefore be well reproduced at higher temperatures, too, because results of the calculation using equation (1) are getting less and less sensitive to the details of the $g(\omega)$ spectrum when the temperature increases.

Our experimental $C_P(T)$ dependence for AlH_3 lies significantly lower than those measured earlier [3, 4]. The calculated $C_V(T)$ dependence is located between ours and the two others, therefore it is likely to represent the heat capacity of AlH_3 more accurately than each of the experimental results.

3.2. High temperatures

Figure 7 shows the behaviour of the heat capacities of α-AlH_3 and α-AlD_3 at temperatures up to 1000 K. Along

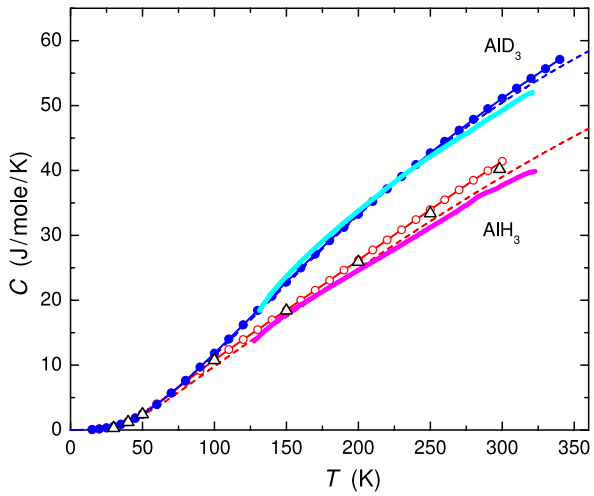

Figure 6. Temperature dependences of the heat capacities of α-AlH_3 and α-AlD_3. The experimental $C_P(T)$ dependences at 130–320 K measured in the present work are shown by the thick solid curves. Other notations as in figure 2.

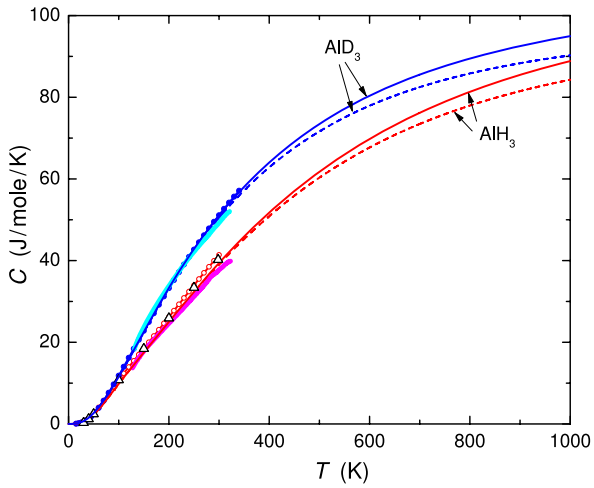

Figure 7. Temperature dependences of the heat capacities of α-AlH_3 and α-AlD_3. The new element compared to the previous figures are the $C_P(T)$ dependences calculated in the present work and shown with the thin solid lines.

with the calculated $C_V(T)$ dependences (dashed lines), the figure depicts the $C_P(T)$ dependences (thin solid lines) also calculated in the present work. While the $C_V(T)$ data are useful for testing the correctness of various theoretical models and *ab initio* calculations of the lattice dynamics, the $C_P(T)$ dependences are necessary for the thermodynamical analysis because they afford the opportunity for the immediate determination of the entropy, enthalpy and free energy of the substance.

In the present work, the $C_V(T)$ dependences were converted to $C_P(T)$ using the equation [12]:

$$\Delta C_{PV}(T) = C_P - C_V = \alpha^2 TV/\beta, \tag{2}$$

where V is the molar volume, $\alpha = (1/V)(\partial V/\partial T)_P$ is the coefficient of volume expansion and $\beta = -(1/V)(\partial V/\partial P)_T$ is the isothermal compressibility. The $C_P(T)$ dependences calculated using (2) were also corrected for the effect of thermal expansion, $\Delta C_{PP}(T)$. The uncertainty in the estimated magnitude of $\Delta C_{PV}(T) + \Delta C_{PP}(T)$ reached about 15 and 25% at 1000 K for α-AlH_3 and α-AlD_3, respectively. At higher temperatures, the uncertainty in the $\Delta C_{PV}(T)$ and $\Delta C_{PP}(T)$ values rapidly increased and this set the upper limit of 1000 K for the temperature range of the $C_P(T)$ dependences considered in the present paper. Note in this connection that a 20% inaccuracy in the $\Delta C_{PV}(T) + \Delta C_{PP}(T)$ value at 1000 K leads to an inaccuracy of about 1 J mol^{-1} K^{-1} or 1% magnitude of the C_P. The $C_P(T)$ dependences presented in figure 7 should therefore be considered nearly as accurate as the $C_V(T)$ ones within the investigated temperature interval 0–1000 K.

Below one can see details of the C_V to C_P conversion.

3.2.1. The V(T) and α(T) dependences. We could not find feasible $V(T)$ or $\alpha(T)$ dependences for α-AlH_3 and α-AlD_3 in the literature and we derived these from an x-ray diffraction investigation at temperatures 80–370 K. Figure 8 presents the experimental data of our work together with the available literature data [10, 13]. As seen from the figure, the results significantly differ for samples from different works and even for the samples from one work [13] prepared by different methods. The origin of this scatter is not known at present. One can speculate that along with the corner-sharing AlH_6 octahedra, which form the ideal α-structure of AlH_3, the α-samples contained a considerable amount of edge-sharing AlH_6 octahedra. The latter are the regular building elements in the crystal structures of six other polymorphic modifications of AlH_3 and their presence decreases the packing densities of those modifications compared to the α-structure (see [13] for references). The defect edge-sharing units would loosen the α-structure and their non-equilibrium concentration would depend on the sample history.

Whatever the reasons of the observed scatter could be, the $V(T)$ dependences constructed in our work were measured using the same α-AlH_3 and α-AlD_3 powders as in the measurements of the inelastic neutron scattering [2] and in the heat capacity measurements, therefore these very dependences are applicable to the case.

To extrapolate our $V(T)$ dependences for α-AlH_3 and α-AlD_3 outside the experimental temperature interval 80–370 K, we made use of the semi-empirical Grüneisen law saying that the coefficient of thermal expansion is approximately proportional to the heat capacity,

$$\alpha(T) = BC_V(T) \tag{3}$$

(see e.g. [12] for discussion). Correspondingly, we wrote

$$V(T) = V(0)\exp\left[B\int_0^T C_V(\tau)\,\mathrm{d}\tau\right] \tag{4}$$

and fitted the experimental dependences with this equation by varying the B parameter. The optimum B-values were 7.84×10^{-7} and 8.19×10^{-7} mol J^{-1}, respectively, for α-AlH_3

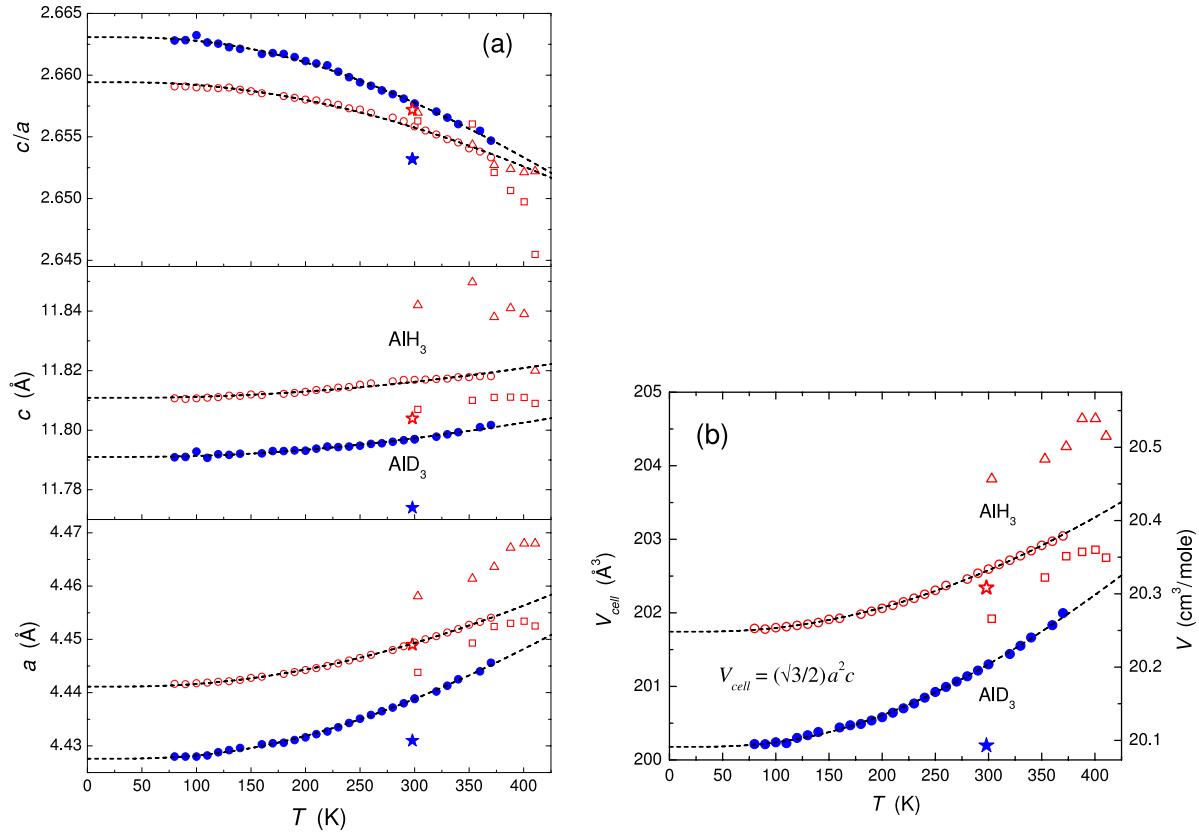

Figure 8. Experimental temperature dependences of the lattice parameters (a) and unit cell volume (b) of α-AlH_3 (open symbols) and α-AlD_3 (solid symbols). The circles show the results of the present work; stars of [10] and triangles and squares of [13]. The triangles are for the α-AlH_3 sample aged under ambient conditions. The squares are for the α-AlH_3 freshly prepared by thermal decomposition of γ-AlH_3. The dashed lines show the results of fitting our experimental data using the Grüneisen law (3).

and α-AlD_3. The resulting fits are shown in figure 8(b) by the dashed curves.

The $a(T)$ and $c(T)$ dependences in figure 8(a) are also fitted using equations analogous to (4). Such a procedure was earlier demonstrated to give accurate values of lattice parameters extrapolated at 0 K for rather anisotropic hexagonal systems [14].

3.2.2. The $\beta(T)$ dependences. Room-temperature values of $\beta_{\text{exp}} = 2.09 \times 10^{-2}$ GPa^{-1} for α-AlH_3 [5] and 2.57×10^{-2} GPa^{-1} for α-AlD_3 [6] are only known from experiment. To take into account the temperature dependence of β in equation (2), one can use another semi-empirical Grüneisen law saying that the dimensionless value of γ defined as

$$\gamma = \frac{\alpha V}{\beta C_V} \tag{5}$$

is weakly dependent on temperature [15]. Using the values of α, V and C_V determined in the present work and the values of β_{exp} taken from [5, 6] gives the Grüneisen constant of $\gamma(298\ \text{K}) = 0.76$ and 0.64 for AlH_3 and AlD_3, respectively. Substituting β from equation (5) into (2), we arrive at [15]:

$$\Delta C_{PV}(T) = \alpha\gamma T C_V. \tag{6}$$

Assuming $\gamma = \gamma\ (298\ \text{K})$ throughout the temperature interval of interest, equation (6) yields $\Delta C_{PV}(T)$ dependences monotonically increasing with temperature (solid curves in figure 9(a)).

The uncertainty in the $\Delta C_{PV}(T)$ values thus calculated can roughly be estimated in the following way.

The consistency of equations (2) and (5) requires the proportionality of β and V:

$$\beta(T) = \beta(0)\frac{V(T)}{V(0)}. \tag{7}$$

Among Grüneisen's empirical and semi-empirical relations there is one

$$(1/\beta)(\partial\beta/\partial T)_P \approx 8.4\alpha$$

(see [16] for discussion and references) that differs from (7) most of all and gives

$$\beta(T) = \beta(0)\left(\frac{V(T)}{V(0)}\right)^{8.4}. \tag{8}$$

From the condition that $\beta(298\ \text{K}) = \beta_{\text{exp}}$ we calculated the $\beta(0)$ values in equations (7) and (8) and constructed the $\beta(T)$ dependences that are plotted in figure 9(b) by the solid and dashed lines, respectively. Substituting the $\beta(T)$ dependences from equations (8) to (2) together with the $\alpha(T)$ and $V(T)$ calculated earlier, we obtained the $\Delta C_{PV}(T)$ dependences

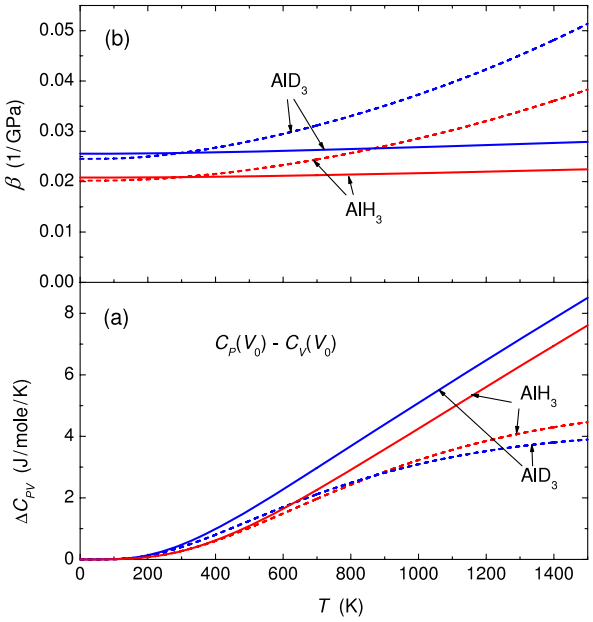

Figure 9. High-temperature extrapolations of (a) the dependences $\Delta C_{PV}(T) = C_P(V_0, T) - C_V(V_0, T)$, where $V_0 = V(9\ \mathrm{K}) \approx V(0\ \mathrm{K})$, and (b) the $\beta(T)$ dependences for α-AlH_3 and α-AlD_3. The solid and dashed curves are calculated assuming, respectively, that equation (7) or (8) is valid (see section 3.2.2).

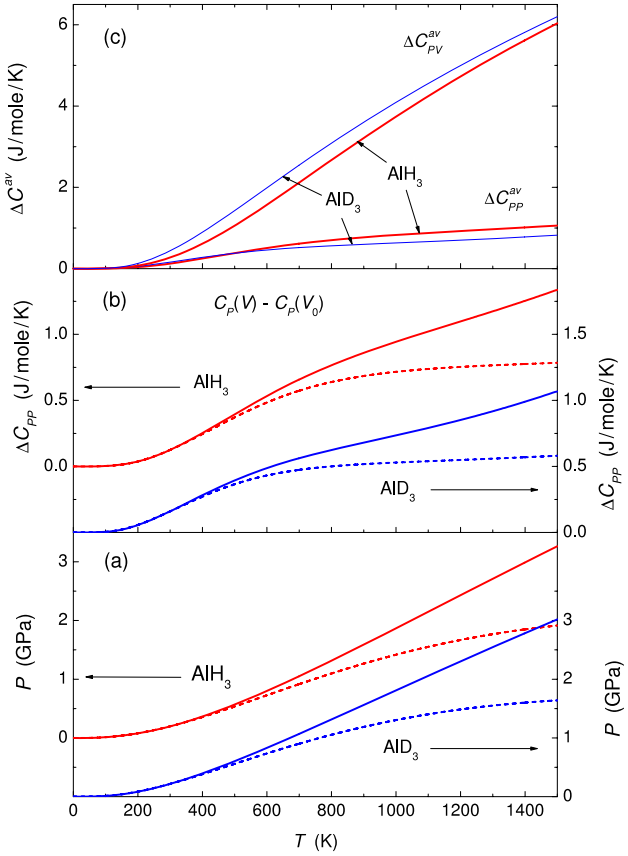

Figure 10. High-temperature extrapolations of (a) the dependences $P(T)$ of the pressure required to compensate for the thermal expansion of α-AlH_3 and α-AlD_3 and (b) the dependences $\Delta C_{PP}(T) = C_P(V, T) - C_P(V_0, T)$. The solid and dashed curves are calculated assuming, respectively, that equation (7) or (8) is valid (see section 3.2.3). The dependences for α-AlH_3 and α-AlD_3 are shifted vertically with respect to each other to avoid overlapping. (c) The arithmetic averages of the $\Delta C_{PP}(T)$ dependences from (b) and of the $\Delta C_{PV}(T)$ dependences from figure 9(a) for α-AlH_3 (thick lines) and α-AlD_3 (thin lines).

shown in figure 9(a) by the dashed curves. As one can see, these dependences significantly depart from those shown by the solid curves, which are calculated using equation (6) and therefore assume that (7) is valid. The true $\Delta C_{PV}(T)$ dependences for AlH_3 and AlD_3 are likely to pass in between the corresponding solid and dashed curves.

3.2.3. The effect of thermal expansion on $C_P(T)$. The $C_V(T)$ dependences calculated in the present work and shown in the figures by the dashed lines refer to the molar volumes V_0 of α-AlH_3 and α-AlD_3 at $T = 9$ K because the phonon densities of states were determined at this temperature [2]. The $C_P(T)$ dependences resulting from equation (2) should therefore be corrected for the thermal expansion of the compounds.

Using the relation [12]

$$\left(\frac{\partial C_P}{\partial P}\right)_T = -T\left(\frac{\partial^2 V}{\partial T^2}\right)_P,$$

the changes in C_P caused by the increase in V with increasing temperature can be estimated as:

$$\Delta C_{PP}(T) = C_P(V, T) - C_P(V_0, T) \approx \left(\frac{\partial C_P}{\partial P}\right)_T (P_0 - P) \approx TP\left(\frac{\partial^2 V}{\partial T^2}\right)_P,$$

where $V(T)$ is given by equation (4), $V_0 = V(9\ \mathrm{K}) \approx V(0\ \mathrm{K})$ at $P_0 = 1$ atm and P is the pressure that reduces the sample volume from $V(T)$ to V_0. The $P(T)$ dependences can be obtained from the equation of state

$$V(P, T) \approx V(T)(1 - \beta P) \qquad (9)$$

under the condition that $V(P, T) = V_0$.

The $P(T)$ dependences calculated using relations (7) and (8) for the compressibility are shown in figure 10(a) by the solid and dashed lines, respectively. At temperatures up to 1000 K, the $P(T)$ values remain in the range of moderate pressures below 2 GPa, so the linear volume dependence on pressure assumed in equation (9) is quite a good approximation for both α-AlH_3 [5] and α-AlD_3 [6].

The calculated $\Delta C_{PP}(T)$ dependences are presented in figure 10(b). One can see that the results of calculations using relations (7) and (8) considerably diverge at high temperatures. Having no reason to prefer one of these relations, we took arithmetic averages of the corresponding pairs of the $\Delta C_{PP}(T)$ dependences shown in figure 10(b) and also of the $\Delta C_{PV}(T)$ dependences from figure 9(a) as the most plausible estimates. The resultant dependences $\Delta C^{\mathrm{av}}_{PP}(T)$ and $\Delta C^{\mathrm{av}}_{PV}(T)$ are presented in figure 10(c). The $C_P(T)$ dependences for AlH_3 and AlD_3 shown in figure 7 by the thin solid lines were calculated as:

$$C_P(V, T) = C_V(V_0, T) + \Delta C^{\mathrm{av}}_{PV}(T) + \Delta C^{\mathrm{av}}_{PP}(T).$$

At temperatures below 1000 K, the additional uncertainty in the determination of C_P compared to C_V does not exceed 1–1.5% and originates mostly from the uncertainty in the estimates of $\Delta C_{PV}(T)$.

3.3. Some useful estimates

The interval of temperatures up to 1000 K is wide enough to make the constructed $C_P(T)$ dependences helpful in the analysis of a large variety of phase equilibria involving AlH_3 and AlD_3. In particular, the equilibrium temperature of the reaction α-$AlH_3 = Al + (3/2)H_2$ in a hydrogen atmosphere monotonically increases with pressure and reaches about 850 K at 6 GPa [17]. This result, in its turn, demonstrates that our extrapolation of the C_P to temperatures 420–1000 K is meaningful despite the decomposition of α-AlH_3 into H_2 gas and Al metal occurring on heating above 420 K at ambient pressure. In fact, concurrently with the steep increase in the Gibbs free energy of the H_2 gas with increasing pressure that stabilizes α-AlH_3 relative to the decomposition, the free energy of α-AlH_3 also increases by a considerable amount of $\Delta G(P,T) = \int_{P_0}^{P} V_{AlH3}(p,T)\,dp$. Nevertheless, the α-AlH_3 phase still remains stable at $P = 6$ GPa at $T \leqslant 850$ K. Having smaller free energy at $P_0 = 1$ atm, α-AlH_3 can therefore exist as a metastable phase at temperatures not lower than 850 K. (Conventionally, the 'phase' means a homogeneous state corresponding to a minimum of the Gibbs free energy at given T and P, and the 'metastable' implies that this minimum is not the deepest one for the given composition of the phase.)

In contrast to the $C_P(T)$ dependences that cannot yet be reliably extended beyond 1000 K, the $C_V(T)$ dependences for AlH_3 and AlD_3 become more and more accurate at higher temperatures because they are approaching a limiting value of $12R \approx 99.77$ J mol^{-1} K^{-1} at $T \to \infty$. An analysis of the $C_V(T)$ dependences in the interval 6–2000 K allows us to estimate the temperature range of applicability of the Debye model (above 1000 K for AlH_3 and 600 K for AlD_3) and establish the precision of the calculated C_V values (no worse than a few per cent for both AlH_3 and AlD_3 at any temperature exceeding 6 K).

3.3.1. The applicability of the Debye model. It is customary to characterize the behaviour of heat capacity of substances with complex crystal structures by the temperature dependence of the Debye temperature, $\theta(T)$, determined from the equation

$$C_V(T) = \nu C_V^{\theta}(T/\theta), \tag{10}$$

where ν is the number of atoms in the formula unit of the substance and

$$C_V^{\theta} = 9R\,(T/\theta)^3 \int_0^{\theta/T} \frac{e^x x^4\,dx}{(e^x-1)^2}$$

is the heat capacity in the Debye approximation [12]. The inset to figure 11 shows the $\theta(T)$ dependences calculated for AlH_3 and AlD_3 with $\nu = 4$.

As seen from the inset, the values of θ rise from 640 to 1940 K for AlH_3 and from 610 to 1460 K for AlD_3 when the temperature increases from 6 to 2000 K. The slopes of the $\theta(T)$ dependences significantly decrease at high temperatures, but still remain large near the upper bound of about 320–370 K of the temperature range where the heat capacity of AlH_3 and AlD_3 can be measured reliably at ambient pressure.

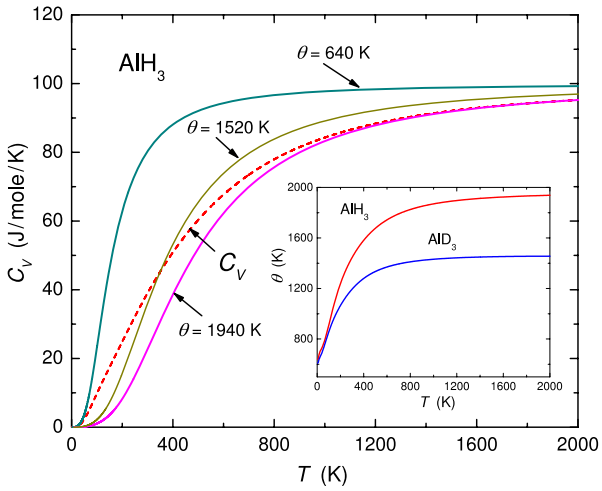

Figure 11. The $C_V(T)$ dependence of α-AlH_3 constructed in this work (dashed curve) and the heat capacities resulting from Debye's model at three different Debye temperatures θ characteristic of α-AlH_3 (solid curves labelled with the θ values). The inset shows the $\theta(T)$ dependences for α-AlH_3 and α-AlD_3 generated by equation (10).

The main frame of figure 11 compares the $C_V(T)$ dependence for AlH_3 constructed in this work with three Debye dependences $4C_V^{\theta}(T/\theta)$ calculated using the extreme values of $\theta = 640$ and 1940 K and also the value of $\theta = 1520$ K corresponding to $T = 350$ K. As one can see, the Debye model is inapplicable to AlH_3 at temperatures up to about 1000 K. At higher temperatures, the $C_V(T)$ dependence for AlH_3 can satisfactorily be described with $4C_V^{\theta}(T/\theta)$ using $\theta \approx 1900$ K.

Similarly, the Debye model fails to reproduce the $C_V(T)$ dependence of AlD_3 at temperatures up to about 600 K and approximates it fairly well at higher temperatures using $\theta \approx 1400$ K.

3.3.2. The accuracy of the C_V calculation. The spectrum of the phonon density of states of α-AlH_3 consists of three well-separated bands. The additive contributions from these bands to the $C_V(T)$ dependence resulting from equation (1) are shown in figure 12.

The integral in equation (1) tends to a limit of

$$C_V^{\infty} = \frac{R}{2}\int g(\omega)\,d\omega$$

when $(\hbar\omega/k_BT) \to 0$. This gives asymptotic values of $C_V^{\infty} = 3R$, $6R$ and $3R$ for phonon bands 1, 2 and 3, respectively, because the areas under the corresponding portions of the $g(\omega)$ curve were normalized to 6, 12 and 6 states in accordance with [11]. Due to the smaller ratio of $\hbar\omega/k_BT$, the contributions to the total $C_V(T)$ from the bands positioned at lower energies approach their limiting values at

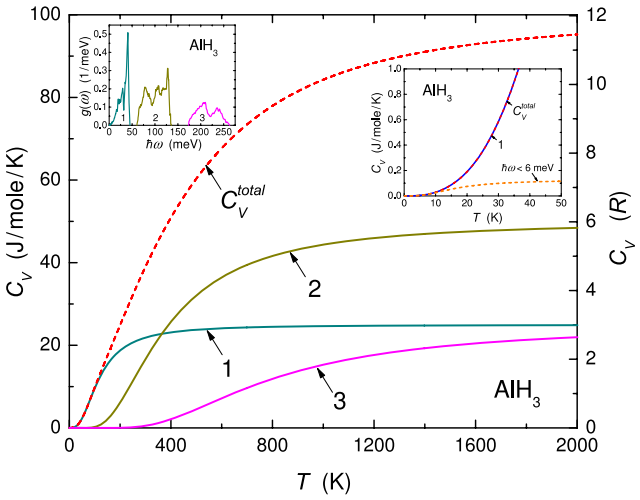

Figure 12. Solid curves 1–3 represent the contributions to the $C_V(T)$ dependence of α-AlH$_3$ (the dashed curve labelled 'C_V^{total}') stemming from the corresponding bands 1 to 3 in $g(\omega)$ shown in the left inset. The right vertical axis is in units of the universal gas constant R. The dashed curve in the right inset demonstrates the small magnitude of the contribution to the $C_V(T)$ from the portion of the $g(\omega)$ below 6 meV that was interpolated by the Debye dependence $g(\omega) \propto \omega^2$ (section 3.1).

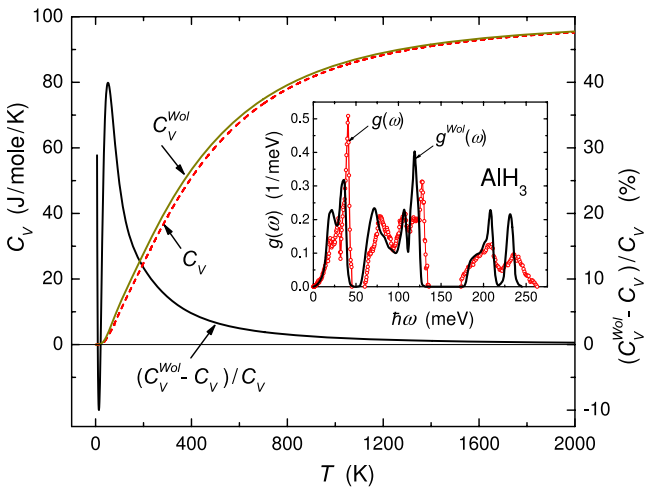

Figure 13. The $C_V(T)$ dependences of α-AlH$_3$ calculated using the $g(\omega)$ spectrum from [2] (dashed curve labelled 'C_V') and [11] (solid curve labelled 'C_V^{Wol}') and the relative error $(C_V^{\text{Wol}} - C_V)/C_V$ in the $C_V^{\text{Wol}}(T)$ dependence (solid curve, right vertical axis). The inset shows the $g(\omega)$ spectra used.

lower temperatures and become weakly sensitive to details and therefore errors in the intensity distribution within the bands. This significantly improves the relative accuracy of the calculation of high-energy parts of the $C_V(T)$ dependence owing to the large contributions from the low-energy phonon bands and causes the errors in these contributions to vanish.

To illustrate what has been said, figure 13 compares $C_V(T)$ dependences calculated for the $g(\omega)$ spectra obtained from the INS experiment [2] and from the *ab initio* calculation by Wolverton *et al* [11]. As seen from the inset to the figure, the intensity distribution is significantly different in all three bands of these $g(\omega)$ spectra. The difference between the resultant $C_V(T)$ dependences is most adequately visualized by the relative error $(C_V^{\text{Wol}} - C_V)/C_V$ shown by the thick solid curve in the main frame of figure 13. The departure of Wolverton's C_V^{Wol} from our C_V values and therefore from experiment is large and irregularly varies with temperature in the range 6–200 K where the $C_V(T)$ behaviour is mostly determined by the shape of the low-energy band of lattice vibrations (see curve 1 in figure 12). At higher temperatures, the relative error in the C_V^{Wol} monotonically decreases. It reaches 5% at 600 K when the increase in the contribution from the lower optical band slows down (curve 2 in figure 12) and falls below 3% at $T > 800$ K.

The magnitude of the $(C_V^{\text{Wol}} - C_V)/C_V$ values in figure 13 overestimates the possible uncertainty in the $C_V(T)$ dependence constructed in the present work because the inaccuracy in the experimental determination of $g(\omega)$ should be much less than the inaccuracy of its *ab initio* calculation. We can therefore conclude that the precision of our $C_V(T)$ dependence for α-AlH$_3$ is better than 5% at 600 K $< T <$ 800 K and better than 3% at higher temperatures. Our dependence agrees with experimental values of the heat capacity of α-AlH$_3$ measured accurate to 2% at temperatures 6–30 K and 5% at 130–320 K (section 3.1). Accordingly, its precision is likely to be within a few per cent at all temperatures above 6 K, including the interval 320–600 K, where direct estimates of the accuracy are difficult.

Since the $g(\omega)$ and $C_V(T)$ dependences for α-AlD$_3$ were constructed in a similar way, its $C_V(T)$ is also expected to be precise within a few per cent at $T > 6$ K.

4. Conclusions

The specific shape of the vibrational spectra composed of three well-separated bands made it possible to accurately determine the heat capacity of α-AlH$_3$ and α-AlD$_3$ over a wide temperature range based on the phonon density of states measured at helium temperatures. In order to facilitate the use of the obtained $C_P(T)$ dependences in the analysis of phase equilibria that involve AlH$_3$ and AlD$_3$ at temperatures up to 1000 K, we also calculated the standard entropy $S^0(T) = \int_0^T \frac{C_P(\tau)}{\tau} \mathrm{d}\tau$, enthalpy $H^0(T) = \int_0^T C_P(\tau)\,\mathrm{d}\tau$ and Gibbs free energy $G^0(T) = H^0(T) - TS^0(T)$ for α-AlH$_3$ and α-AlD$_3$. These dependences together with the $C_V(T)$ and $C_P(T)$ ones are available in numeric format at stacks.iop.org/JPhysCM/20/275204.

Acknowledgments

This work was supported by grant No. 08-02-00846 from RFBR, by the Programme 'Physics and Mechanics of Strongly Compressed Matter' of RAS, and by the INTAS Project No. 05-1000005-7665. Work at ANL was performed under the auspices of the US DOE-BES, Contract No. DE-AC02-06CH11357.

References

[1] Goncharenko I N, Eremets M I, Hanfland M, Tse J S, Amboage M, Yao Y and Trojan I A 2008 *Phys. Rev. Lett.* **100** 045504

[2] Kolesnikov A I, Antonov V E, Markushkin Yu E, Natkaniec I and Sakharov M K 2007 *Phys. Rev.* B **76** 064302

[3] Sinke G C, Walker L C, Oettings F L and Stull D R 1967 *J. Chem. Phys.* **47** 2759–61

[4] Gavrichev K S, Gorbunov V E, Bakum S I, Gurevich V M and Izotov A D 2002 *Inorg. Mater.* **38** 661–4

[5] Baranowski B, Hochheimer H D, Strössner K and Hönle W 1985 *J. Less-Common Met.* **113** 341–7

[6] Goncharenko I N, Glazkov V P, Irodova A V and Somenkov V A 1991 *Physica* B **174** 117–20

[7] Brower F M, Matzek N E, Reigler P F, Rinn H W, Roberts C B, Schmidt D L, Snover J A and Terada K 1976 *J. Am. Chem. Soc.* **98** 2450–3

[8] Palnichenko A V, Gurov A F, Kopylov V N, Kusano K, Tanuma S and Salamatov E I 1997 *Phys. Rev.* B **56** 11629–34

[9] Larson A C and Von Dreele R B 2004 General structure analysis system (GSAS) *Los Alamos National Laboratory Report LAUR* pp 86–748

[10] Turley J W and Rinn H W 1969 *Inorg. Chem.* **8** 18–22

[11] Wolverton C, Ozoliņš V and Asta M 2004 *Phys. Rev.* B **69** 144109

[12] Landau L D and Lifshitz E M 1980 *Statistical Physics, Part 1* 3rd edn (Oxford: Pergamon)

[13] Maehlen J P, Yartys V A, Denys R V, Fichtner M, Frommenc Ch, Bulychev B M, Pattison P, Emerich H, Filinchuk Y E and Chernyshov D 2007 *J. Alloys Compounds* **446/447** 183–7

[14] Sayetat F, Fertey P and Kessler M 1998 *J. Appl. Crystrallogr.* **31** 121–7

[15] Grüneisen E 1908 *Ann. Phys.* **26** 394–402

[16] Fürth R 1941 *Proc. Camb. Phil. Soc.* **37** 34–54

[17] Konovalov S K and Bulychev B M 1995 *Inorg. Chem.* **34** 172–5